

Depth-AGMNet: an Atrous Granular Multiscale Stereo Network Based on Depth Edge Auxiliary Task

Weida Yang¹, Yong Xu, Yong zhao

¹Association for the Advancement of Artificial Intelligence

2275 East Bayshore Road, Suite 160

Palo Alto, California 94303

publications20@aaai.org

Abstract

Recently, end-to-end convolutional neural networks have achieved remarkable success in stereo estimation tasks. It is still a valuable but hard problem to find the correct correspondence for the ill-posed regions, such as texture-less areas, edge details, and small objects. Based on the above questions, this paper proposes Dedge-AGMNet to alleviate it in different methods. First, we present the multi-task network composes of a depth-edge auxiliary network and disparity estimation network. To fuse the information of the ancillary system effectively, we design Dedge-SPP to embed the depth edge contours. Besides, On the supervised and unsupervised tasks of the depth edge, the corresponding loss function is constructed for depth edge constraints. Second, we design the AGM module, which utilized the fusion of internal fine-grained feature and stacking convolution layers within a single layer, combining with the dilated convolution and parallel structure reasonably. It is beneficial to provide dense -scale receptive fields and potential correspondence. The results show that for the unsupervised task of depth edge, the network can optimize the edge effectively. Our proposed approach shows accurate disparity estimates and achieves state-of-the-art performances on Sceneflow, KITTI2012, and KITTI2015 benchmarks datasets.

1. Introduction

Depth estimation based on stereo vision is a fundamental research aiming to predict the distance between the pixel of the objected scene with the camera. It has various essential applications, such as autonomous driving, dense reconstruction and robot navigations. As a kind of passive depth sensing techniques, stereo matching estimates disparity from rectified image pairs with camera calibration. For each pixel in the left image, its corresponding pixel can be found in the right image on the same horizontal line so that the pair of pixels are the projections of a same 3D position.

The traditional stereo estimation is divided into four steps, namely feature extraction, matching cost computation, disparity aggregation and computation, and an optional disparity refinement. With the development of deep learning, CNN-based disparity estimation systems take their cues, and

constitute of different modules that attempt to perform the same tasks. However, there are many shortcomings in the early CNN-based methods, such as discontinuous inference process, limited receptive field, and using post-processing functions that are hand-designed. The end-to-end disparity estimation network is proposed to integrate all the steps for joint optimization. Nowadays, It has been proved to be a valid architecture composed of 3D convolutions(Chang and Chen 2018; Kendall et al. 2017).

However, even for the state-of-the-art stereo networks, it is still difficult to find corresponding matching points in ill-posed regions of the image, such as texture-less areas, edge details, small objects, and so on. Its still a valuable but hard challenge to capture correct matching points in these regions. Currently, there are two main methods for optimizing this regions. The first one is that some networks utilize a set of stacked 3D convolution modules (Chang and Chen 2018; Du, El-Khamy, and Lee 2019) or parallel structure (Chabra et al. 2019) to capture potential correspondence relationship. It greatly increases the computational consumption and memory footprint. Second, Some networks remain the high-frequency representation of images by means of auxiliary networks (Yang et al. 2018a; Song et al. 2019; Du, El-Khamy, and Lee 2019), such as semantic segmentation, edge detection, and fore-background awareness networks. However, the semantic segmentation feature will blur the depth features of the overlapping objects with the same kind. The standard edge information contains a large number of noise edges, such as object inner patterns. These noise edges cause misjudgment of the disparity estimation.

In view of the above problems, this paper proposes an effective multi-task learning network Dedge-AGMNet, which effectively alleviate the drawbacks of both methods to gain an accuracy result. We first design the depth edge auxiliary network to capture geometric contour and provide edge constrain. By re-extracting the shared features to obtain the high-frequency and the semantic information in different methods. And both of them are merged through shared concatenation to predict depth edge. Compared with traditional edge detection, the network we proposed reduce noise edge heavily. The depth edge can be abstracted as binary information of the semantic edge, but it ignores the edge-specific seman-

tic information to ease the task difficulty. Meanwhile, the depth edge detection sub-network could take more attention to geometric information and fine-grain presentation.

Second, this paper proposes a novel module , AGM (atrous granular multiscale) module. Refer to Res2net(Gao et al. 2019), we present the granular convolution,which divides the feature of a single layer into multiple groups and take the convolution and accumulation iteratively at more granular level. By combining the parallel structure and selecting the suitable parameters of the dilated rate, AGM module is designed to contain dense receptive field with less parameters and computation consumption. The main contributions are summarized as follows:

- We first propose the depth edge auxiliary network to provide geometric structure and fine grain presentation for disparity estimation. And the correspond loss function provides edge constraints for the shared feature extraction module.
- The AGM module is designed to capture the dense scale information of 3D aggregation for potential correspond relationship with less parameters and computational cost.
- Our method achieves state-of-the-art accuracy on the Sceneflow dataset, KITTI 2012 and KITTI2015 stereo benchmarks.

2.Related work

Depth from stereo has been widely studied for a long time in the literature, and we refer the interested reader to surveys and methods. The traditional stereo matching methods(Schops et al. 2017) have been proposed for four steps: matching cost computation(Zbontar, LeCun, and others 2016), cost aggregation(Luo, Schwing, and Urtasun 2016), optimization(Seki and Pollefey 2017; ?), and disparity refinement. Recently, convolutional neural network have become popular in solving this problem, which achieve the state-of-the-art performance. Zbontar and LeCun(Zbontar, LeCun, and others 2016) are the first to use CNN for matching cost computation. Luo et al.(Luo, Schwing, and Urtasun 2016) designed a noval Siamese network to treat the computation of matching cost as a multi-label classification, which compute the inner product between the left and the right feature maps. Seki et al.(Seki and Pollefey 2017) raised the SGM-Net that predicts SGM penalties for regularization.

Inspired by other pixel-wise labeling tasks, the end to end neural networks has been proposed using the fully-convolution network(Long, Shelhamer, and Darrell 2015) for stereo disparity estimation. Mayer et al(Mayer et al. 2016) designed the first end-to-end disparity estimation network called DispNet, which using the encoder-decoder structure with short-cut connections for second stage processing. Kendall et al(Kendall et al. 2017) raised GCNet, a cost volume formed

by concatenating the feature maps to incorporates contextual information, and applied the 3D encoder-decoder architecture to regularize the cost volume. In order to find correspondence in ill-posed regions, CHang and Chen(Chang and Chen 2018) proposed the PSMNet to regularize cost vol-

ume using stacked multiple hourglass networks in conjunction with intermediate supervision. Each hourglass CNN has an encoder-decoder architecture, and the encoder parts particulate downsampling of the cost volume while the decoder parts involve upsampling of it.

Currently, Chabra(Chabra et al. 2019) proposed a depth refinement architecture that help fusion system to produce geometrically consistent reconstructions, and utilize 3D dilated convolutions to construct hourglass architecture. Meanwhile, Xianzhi Du et al(Du, El-Khamy, and Lee 2019) designed an similar construction with three atrous multiscale modules, while is useful to aggregate rich multi-scale contextual information from cost volume. The paper also fusion the ResNet and the depth-separable convolution to make a new block,D-ResNet, to learn more deep features. Base on the PSMNet(Chang and Chen 2018), both of them achieve the state of the art on the varity dataset.

Multi-scale features is an important factor to pixel-predicted task such as segmentation and stereo estimation, while ambiguous pixels requiring diverse range of contextual information. ASPP(Chen et al. 2017) are designed to concatenate various features map with different receptive field size. To further quest the importance of receptive field, Yang et al.(Yang et al. 2018b) proposed Dense ASPP to concatenates a set of different atrous convolutional layers in a dense way, which also encourage feature reuse because of the similarity with the Dense Net(Huang et al. 2017). Instead of representing the multi-scale features in a layer wise manner, Gao et al.(Gao et al. 2019) designed novel architecture, namely Res2Net, by using hierarchical residual-like connections in a single block to represent it at a granular level. With the same computational resources as ResNet block, Res2Net achieve more accurate results.

Focus on improving the accuracy in the regions where single stereo estimation network are difficult to estimate, such as non-textures regions, boundaries regions and so on. Yang et al.(Yang et al. 2018a) proposed SegStereo to embed the semantic feature, and regularizes semantic cues as the loss term. Xianzhi Du et al(Du, El-Khamy, and Lee 2019) utilize foreground-background segmentation map to improve disparity estimation because the better awareness of foreground object will lead to a more accurate estimation. Song et al.(Song et al. 2018; Song et al. 2019) proposed EdgeStereo which compose a disparity estimation sub-nework and an edge detection sub-network. By combining the advantages of the semantic segmentation and edge detection, we first proposed an efficient disparity estimation network that combines depth edge detection sub-network.

3.Algorithm

We propose Dedge-AGMNet, compose of a depth edge branch and a disparity estimation branch. The depth edge sub-network provides geometric knowledge and constraints without adding unrelated edges.We design a more efficient 3D aggregate filtering module with the granular convolution. And get richer features by simply gathering the cost volumes constructed by two common modes.

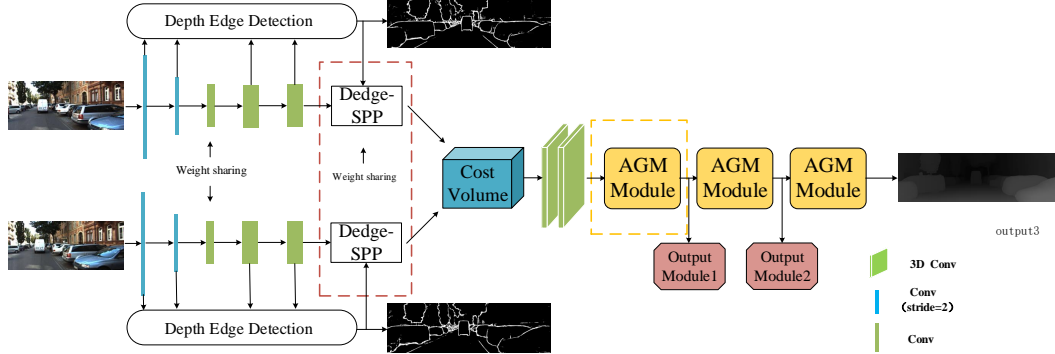


Figure 1: The pipeline of the proposed depth edge-Atrous Granular Multi-scale context Network(Dedge-AGM Net).

3.1. Network Architecture

The structure of the proposed Dedge-AGMNet is shown in 1. The network consists of five parts, feature extraction, depth edge prediction and embedding, cost volume construction, 3D aggregation and disparity prediction.

For the shared feature extraction about both sub-network, we remain the ResNet-like structure used in PSMNet except downsampling at the beginning of the network. Three convolution filters(3×3) with stride=1 are cascaded to obtain lossless frequency information, which is indispensable for semantic edge network.

The depth edge by nature is an unary representation of the semantic edge. We present the depth edge sub-network with D_{edge} or smoothness loss functions to provide geometrically constraint for the share features. Beside, Instead of SPP(Chang and Chen 2018), Dedge-SPP module is constructed to fuse the information from feature extraction and depth edge branch. And details are described in Section 3.2.

The cost volume is consisted of two parts, a concatenation volume and a distance volume. We process the cost volume with a pre-hourglass module and three stacked AGM modules. As shown in figure 1, the pre-hourglass module consists of a set of stacked CNN layers. Three stacked AGM module are followed to capture dense scale information. And details are described in Section 3.3.

The depth edge branch is connected to an output module. Similarly, for the disparity estimation sub-network, three stacked AGM modules are connected to output modules to

predict disparity maps. The details of the output modules and the loss function are described in Section 3.4.

3.2. Cooperation of Edge Cues

Structure of the depth edge sub-network Without the geometric knowledge and constraints, it's difficult to match correct correspondence in ill-regions regions. The classical edge branch is beneficial but it captures much edge noise, such as object pattern, inner edges. These un-semantic information disturbs the disparity estimation heavily. And Semantic segmentation sub-network are commonly used, it provides semantic information correctly, but it meets the similar problem with the disparity estimation, not optimize for each other like edge detection task.

Based on the above-mentioned drawbacks, we first propose the depth edge auxiliary network, which is an end-to-end sub-network architecture that shares the feature extraction module with disparity estimation. Refer to CASENet, the depth edge branch is adopted a nested architecture but also contains several key modifications.

Aiming at providing geometric features for the disparity estimation sub-network, we utilize the same feature extraction module for the depth edge branch and the stereo estimation branch. We take the feature re-extraction module for the bottom side features to compress them. Meanwhile, we add the conv5 module to capture high-level features, and employ the A5 module to handle K channels for top side features. Compared with bottom features, more channels mean

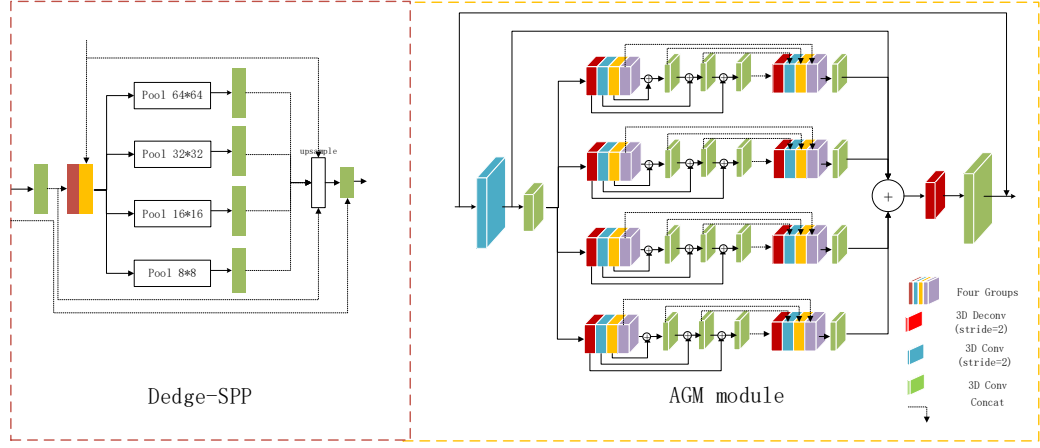


Figure 2: the architure of out proposed Dedge-SPP and AGM module.

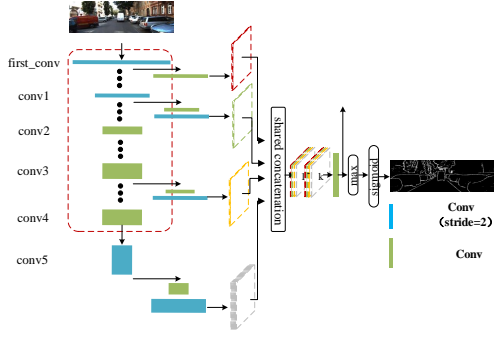


Figure 3: The architecture of the depth edge brach. And the red dashed box shows the shared feature extraction between sub-networks.

greater importance .At last, the shared concatenation is applied to fuse all features, then we compress and normalize the fused features to predict the label of each pixels. The specific structure is shown in 3.

The bottom features $F = \{F(1), F(2), F(3)\}$ comes from feature re-extraction modules, the top features with K channels is represented by A5. And the shared concatenation as follows:

$$A5(1), F, A5(2), F, \dots, A5(K), F$$

Different with CASENet, We simplify the task into binary depth edge prediction, which not only take attention to the target edge, but also reduces the task difficulty.Besides, by reducing channels for sharing feature extraction modules, Auxiliary networks decrease parametric redundancy and computational consumption greatly.

Dedge-SPP We incorporate depth edge cues in two methods. The first one is the Dedge-SPP (depth edge atrous spatial pyramid pooling). As shown in 2, we fuse the features from two branches to modify the SPP. And the Dedge-SPP

was designed to share the geometric knowledge with the disparity estimation branch.

L_{edge} and L_{smooth} Since the depth edge label is a binary representation, for supervised tasks, we use Binary Cross Entropy instead of the multi-label loss(Yu et al. 2017) .It denoted as L_{edge} . $P(X_i; W)$ is the predict probability for the image pixel X_i .As shown in eq1,

$$L_{edge}(X_i, W) = \begin{cases} \alpha * \log(1 - P(X_i; W)), & \text{if } y_i = 0 \\ \beta * \log P(X_i; W), & \text{if } y_i = 1 \end{cases} \quad (1)$$

in which

$$\alpha = \frac{|Y^+|}{|Y^+| + |Y^-|} \quad (2)$$

$$\beta = \frac{|Y^-|}{|Y^+| + |Y^-|}$$

For unsupervised networks, this paper proposes a depth edge-aware smoothness loss, denoted as L_{smooth} . We encourage it could penalty drastic depth changes in flat regions. Previous weight smoothness regularization terms(Zbontar, LeCun, and others 2016; Zhong, Dai, and Li 2017) based on the image gradient, which change sharply to various lighting conditions. Edgestereo(Yang et al. 2018b) improves the performance based on the edge gradient, it still mixed with some non-semantic edges.Compared with the previous methods, The depth edge gradient is more consistent with the change of the disparity map.

$$L_{sm} = \frac{1}{N} \sum_{i,j} |\partial_x d_{i,j}| e^{-\beta |\partial_x \xi_{i,j}|} + |\partial_y d_{i,j}| e^{-\beta |\partial_y \xi_{i,j}|} \quad (3)$$

where N denotes the number of pixels, and ∂d and $\partial \xi$ present the disparity and the depth edge map grandient respectively. β is hyper-parameter.

3.3 atrous granular multiscale module

Inspire by Res2Net(Gao et al. 2019) and ASPP(Chen et al. 2017), we propose AGM-module, which combines the advantages of layer-wise manner and granular level.Except

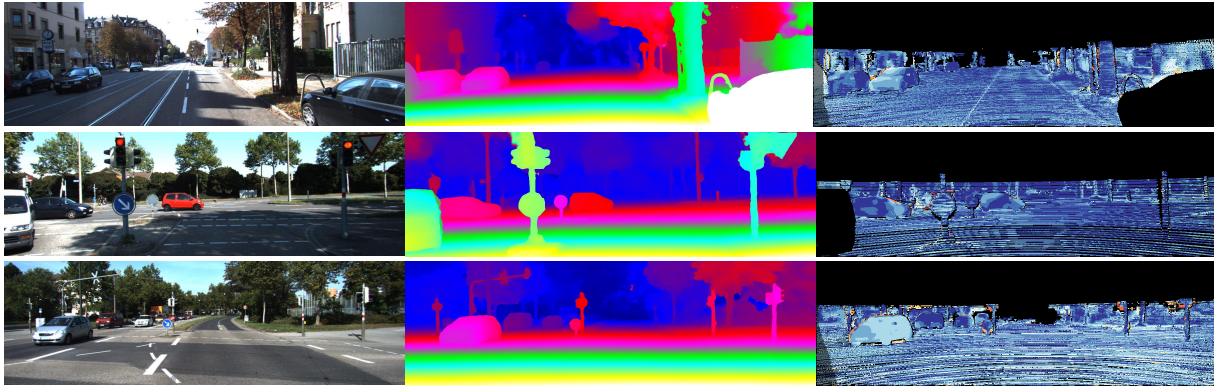


Figure 4: Results on the KITTI 2015 test sets. From left: left stereo image, disparity map, error map.

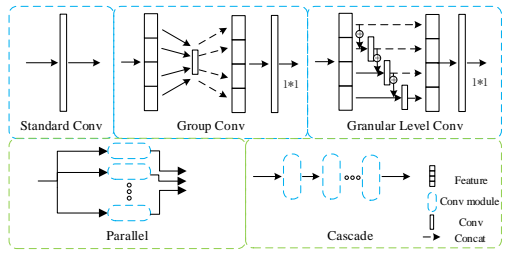


Figure 5: The blue dashed boxes show the simplified diagram of different kind of convolutions, including standard convolution, dilated convolution, and granular convolution. And blue dashed boxes present the parallel and cascade structures.

some essential operators like updown sampling and shortcut connection, the main part of this module is the parallel structure with four granular convolution(dilated rate = 1,4,8,16). The granular convolution divides input features into several groups, and output features of the previous group are then sent to the next group of filters alone with another group of input feature maps. All the features are aggregated by pointwise convolution. And the detail are described in Fig.2.

Compared with the cascade or parallel structure of other convolution filter, granular convolution in parallel take both of their advantages. Not only gain more scale context information than both of them, it also capture a larger scale receptive field and lead more pixels involved in convolution.

Formally, For the three convolutions below, we define some common attributes. W denotes weight, c denotes the number of channels, s denotes the kernel size of convolution, and the dilated rate denotes a . Besides, we ignore some irrelevant operators, such as the biases, batch norm, and the activation function. The convolution is added to image features v to obtain v' . \times denotes the convolution operator.

Spatial convolution:

$$v' = W \times v; \quad W \in R_{c*c*s*s} \quad (4)$$

For group and granular convolutions, G is the number of

groups, \sum denotes the concatenation operator. The pointwise convolution $W^1 \in R_{c*c*1*1} \quad v = (v_1, v_2, \dots, v_G)$
Group convolution:

$$v' = W^1 \times \left(\sum_{g=1}^G W_g \times v_g \right) \quad (5)$$

where $W = (W_1, W_2, \dots, W_G)$, and $W_1 = W_2 = \dots = W_G$. $W \in R_{\frac{c}{G} * \frac{c}{G} * s * s}$.
Granular convolution:

$$\begin{aligned} \hat{v}'_1 &= W_1 \times v_1 \\ \hat{v}'_2 &= W_2 \times (v'_1 + v_2) \\ &\dots \\ \hat{v}'_G &= W_3 \times (v'_{(G-1)} + v_G) \end{aligned} \quad (6)$$

From eq6, v' is shown follow:

$$\begin{aligned} v' &= W^1 \times \left(\sum_{g=1}^G \hat{v}'_g \right) \\ &= W^1 \times \left(\sum_{g=1}^G \sum_{i=1}^g W_1 \times \dots \times (W_i \times v_{(g-i)}) \right) \end{aligned} \quad (7)$$

where $W = (W_1, W_2, \dots, W_G)$, and $W_1 \neq W_2 \neq \dots \neq W_G$. $W \in R_{\frac{c}{G} * \frac{c}{G} * s * s}$.

The above convolution operator can be represented by the function F . K denotes the number of convolution layers. It is straightforward to present the cascade and parallel structure as follow:

- the cascade structure: $v' = F_k \times \dots \times (F_1 \times v)$
- the parallel structure: $v' = \sum_k^K (F_k \times v)$

After Substitute Eq(4), Eq(5) and Eq(6) into the above equation respectively, we get the most reasonable structure, parallel granular convolution with different dilated rate.

$$v' = \sum_k^K \left(W^1 \times \left(\sum_{g=1}^G \sum_{i=1}^g W_1 \times \dots \times (W_i \times v_{(g-i)}) \right) \right) \quad (8)$$

The above formulas show that the number of receptive fields in granular convolution is about G times than other

convolutions in parallel. Its $G * K$ times than the spatial convolution in cascade. It's known that the dilated convolution gradually loss its modeling power as the dilation rate increases ($d > 24$) .(Chen et al. 2017) As seen from $W_1 * W_2 \dots * W_i$ in Eq8, with the internal cascade structure of granular convolution, AGM module are able to cover the large scale range in a dense manner. Besides, This module reduces computational costs and save the number of parameters, the detail will be showed in Section 4.

3.4. Gathered cost volume(GCV)

We design the cost volume by stacking the distance module and the concatenation module. The former provides the overall information of the features, which is formed by concatenating left feature maps with their corresponding right feature maps[GCNet].and the latter take the difference between the two across each disparity level to provide feature similarity information.

3.5. Output module and loss function

The output module has the similar architecture as PSMNet, containing two stacked 3D convolution layers and the upsample operator. And the volume c_d from output module is converted into a probability volume with softmax function $\sigma(\cdot)$ along the disparity dimension. The predicted disparity \hat{d} is calculated as follow:

$$\hat{d} = \sum_{d=0}^{D_{max}} d \times \sigma(-c_d)$$

The predicted disparity maps from three output modules are denoted as $\hat{d}_1, \hat{d}_2, \hat{d}_3$, The L_{disp} is given:

$$L_{disp} = \sum_{i=1}^3 \lambda_i * Smooth_{L_1}(\hat{d}_i - d^*) \quad (9)$$

where λ denotes the coefficients and d^* represents the ground-truth disparity map.

For supervised network of depth edge, Combined with Eq(1) and Eq(9),

$$L_{total} = L_{disp} + a_s * L_{edge}$$

For unsupervised network, Combined with Eq(2) and Eq(9),

$$L_{total} = L_{disp} + a_{un} * L_{smooth}$$

4.Experiment

In this section, we will train our proposed model in Sceneflow, cityscapes and KITTI datasets, and only evaluate it on Sceneflow and KITTI datasets. Because the disparities of Cityscapes dataset are obtained by SGM algorithm, but not the groundtruth. The datasets and network implementation are presented in Section 4.1 and Section 4.2. The ablation studies to compare different modules and different parameter settings are discussed in Section 4.3 and Section 4.4. We present optimal depth edges with L_{smooth} in Section 4.5. Followed by the evaluation results on the datasets.

4.1. datasets and evalution metric

Sceneflow: a large scale synthetic dataset contain three sub-set(Flyingthings3D, Driving and Monkaa),which provides about 35000 training and 4000 testing stereo image pairs of size 960*540. It consists of left and right images, complete ground-truth disparity maps and segmentation images. With segmentation images, We generate the semantic edges and then binarize it into ground-truth depth edges. The end-point-error (EPE) is used as the evaluation metric.

Cityscapes: an urban scene understanding dataset. This dataset provides 3475 rectified stereo pairs, fined annotated segmentation maps and their corresponding disparity maps precomputed by SGM algorithm. We generate the ground-truth depth edges with the same method.

KITTI 2012 and KITTI 2015:both of them are driving scene datasets. KITTI 2012 provides 194 training and 195 testing image pairs. KITTI2015 contains 200 training and 200 testing image pairs. With the size of 1240*376, both the datasets provide sparse ground-truth disparity maps. We divide the whole training data and remain 20 image pairs as the validation set. The main evaluation metric for KITTI2015 is D1-all error, which computes the percentage of pixels for which the estimation error is $\geq 3px$ and $\geq 5\%$ of its ground-truth disparity. The main evaluation criterion for KITTI 2012 is Out-Noc, c which computes the percentage of pixels for which the estimation error is $\geq 3px$ for all non-occluded pixels.

4.2.Network implementation

The Dedge-GAMNet architecture is implement with PyTorch. All models are trained with Adam optimizer($\beta_1 = 0.09, \beta_2 = 0.999$). We use 4 Nvidia TITAN XP GPUS training models, and the batch size is fixed to 8. The images are randomly Crop to size 512*256. The coefficients of disparity outputs are set as $\lambda_1 = 0.5, \lambda_2 = 0.7, \lambda_3 = 1.0$. For depth edge outputs, $\beta = 2$ (Song et al. 2019), $a_s = 1, a_{un} = 0.5$. For the training process, we combined Sceneflow and Cityscapes(repeat fifteen times) datasets to learn the accurate disparity result and the depth edge of unban scene simultaneously. We adopt a learning strategy as like GWC(Guo et al. 2019), the initial learning rate is set to 0.001, and it is down-scaled by 2 for every 2 epoches until epoch 16. The maximum disparity (D_{max}) is set to 192. For KITTI,we fine-tuned the pre-trained model for 300 epochs. The initial learning rate is set to 0.001 and is reduced to 0.0001 after epoch 200. For feature re-extraction module of the auxiliary network,we set the learning rate to 1/1000 of the main network to avoid learning excessively. Further, we prolonged the training process to 1000 epochs to obtain the final results for KITTI submission.

4.3.The effectiveness of AGM module

Experiment results in Table 1 show that the parallel structure with one more granular convolutions can achieve better results while the dilated rate in an appropriate range. Besides, the results present that as the dilated rate increases, the performance improving gradually until the maximum dilated rate reaches 16. We conclude that the AGM module with a



Figure 6: From left: image in the KITTI 2015 training set, depth edge from the pretrained sub-network, depth edge after multi-task learning.

Model	hourglass	Dilation rate				FLOPS	Paramters	Sceneflow(EPE)
PSM_ours	[PSM]	-				33.79GMac	540.7k	0.889
AGM148-base	AGM module	1	4	8	-	23.65GMac	126.8k	0.836
AGM1234-base	AGM module	1	2	3	4	24.02GMac	133.0k	0.823
AGM1248-base	AGM module	1	2	4	8	24.02GMac	133.0k	0.821
AGM14816-base	AGM module	1	4	16	32	24.02GMac	133.0k	0.842
AGM141632-base	AGM module	1	4	8	16	24.02GMac	133.0k	0.801

Table 1: PSM_ours represents a similar structure with PSMNet except replacing 4 convolution layers in feature extraction, and it has similar accuracy. AGM_base network is defined to the model that only replaces the hourglass structure of PSM to AGM module. All models are trained with the same learning strategy. FLOPS are measured on the stereo pairs of Sceneflow dataset.

Modes	hourglass	CV	Dedge	SPP	Sceneflow	KITTI2015
PSM_ours	-	-	-	-	0.884	1.67
AGMNet	AGM	-	-	-	0.801	1.62
AGMNet	AGM	GCV	-	-	0.754	1.56
Dedge-AGMNet	AGM	GCV	Ours	-	0.663	1.42(un)
Dedge-AGMNet	AGM	GCV	Ours	Ours	0.645	1.38(un)

Table 2: Ablation study on Sceneflow test and KITTI 2015 validation set. '-' means the network has the same module as PSMNet, and it denotes none if PSMNet has not the module. (un) indicates it is an unsupervised task of depth edge.

dilated rate of 1, 4, 8, 16 could provide optimal performance. All the AGM-base networks outperform PSMNet. And with the best setting of the AGM module, The EPE is reduced by 9.3% and the computational consumption is only () of initial hourglass structure.

4.4. The effectiveness for depth edge sub-network

As shown in Table 2, the loss function we proposed is useful for supervised or unsupervised sub-network of depth edge. Undoubtedly, the supervised one provide more accurate cues and achieve more improvement. As listed in Table 5, Dedge-SPP works better while the architecture fuses the features between the branches. In summary, Dedge-AGM model significantly outperformed the basic model when combined with GCV module and AGM module.

We perform an ablation study for the other module, it presents that the module we proposed has a certain effect on network promotion. Compared to PSM_ours, our proposed network has a 27.0% reduction in EPE on the Sceneflow and 17.4% on the KITTI2015 validation dataset. As shown in Fig.5, after multi-task learning in the KITTI 2015 train-

ing set, depth edge prediction significantly refined without ground-truth depth edge annotations. It shows that the depth edge-aware smoothness loss is not only effective for disparity estimation, but also improves the effect of depth edges.

4.5.Result

We compared the performance of the Dedge-AGMNet with other state-of-the-art methods. For Sceneflow, the Dedge-AGMNet we proposed reduced EPE to 0.645, which outperform other published methods significantly. As shown in Table 4 and Table 5, integrating the ranks of KITTI2012 and KITTI2015, The Dedge-AGMNet achieves the best accuracy compared to all multi-task learning models. Fig.4 gives qualitative results on the KITTI test sets. Our proposed approach achieves state-of-the-art performances on Sceneflow, KITTI2012 and KITTI2015 benchmarks datasets, it demonstrates the powerful generalization performance of this model.

5. Conclusions

In this paper, we proposed the Dedge-AGMNet, a multi-task learning network for disparity estimation and depth edge detection. It consists of two main modules to reduces the error in ill-posed regions: Depth edge sub-network and AGM module. To effectively incorporate depth edge cues, we design Dedge-SPP and propose the corresponding loss for supervised or unsupervised auxiliary tasks. The AGM module provides dense scale context information with less computational consumption. In our experiment, the approach we proposed achieve state-of-the-art performances, and outperforms other multi-task learning models on Sceneflow dataset, KITTI 2012 and 2015 benchmarks. We provide qualitative demonstrations that depth edge prediction are

Method	All(%)			Non-Occluded(%)			Runtime (s)
	D1-bg	D1-fg	D1-all	D1-bg	D1-fg	D1-all	
GC-Net	2.21	6.16	2.87	2.02	5.58	2.61	0.9s
PSMNet	1.86	4.62	2.32	1.71	4.31	2.14	0.41s
SegStereo	1.88	4.07	2.25	1.76	3.70	2.08	0.6s
EdgeStereo	1.84	3.30	2.08	1.69	2.94	1.89	0.32s
AMNet	1.53	3.43	1.84	1.39	3.20	1.69	0.9s
Dedge-AGMNet	1.54	3.37	1.85	1.41	2.98	1.67	0.9s

Table 3: Comparison with the top publicized methods on the KITTI stereo 2015 test set.

mthod	> 2px(%)		> 3px(%)		> 4px(%)	
	Noc	All	Noc	All	Noc	All
GC-Net	2.71	3.46	1.77	2.30	1.36	1.77
SegStereo	2.66	3.19	1.68	2.03	1.25	1.52
PSMNet	2.44	3.01	1.49	1.89	1.12	1.42
AMNet	3.12	2.71	1.32	1.73	0.99	1.31
EdgeStereo	2.32	2.88	1.46	1.83	1.07	1.34
ours	2.02	2.56	1.26	1.64	0.95	1.24

Table 4: Comparison with the top publicized methods on the KITTI stereo 2012 test set.

method	EPE	method	EPE	method	EPE
GC-Net	2.51	SegStereo	1.45	PSMNet	1.09
CSPN	0.77	AMNet	0.74	ours	0.645

Table 5: Comparison with the top publicized methods on the Sceneflow test set.

improved after multi-task learning even without the corresponding ground-truth annotations for training.

References

[Chabra et al. 2019] Chabra, R.; Straub, J.; Sweeney, C.; Newcombe, R.; and Fuchs, H. 2019. Stereodrnet: Dilated residual stereonet. In *Proceedings of the IEEE Conference on Computer Vision and Pattern Recognition*, 11786–11795.

[Chang and Chen 2018] Chang, J.-R., and Chen, Y.-S. 2018. Pyramid stereo matching network. In *Proceedings of the IEEE Conference on Computer Vision and Pattern Recognition*, 5410–5418.

[Chen et al. 2017] Chen, L.-C.; Papandreou, G.; Schroff, F.; and Adam, H. 2017. Rethinking atrous convolution for semantic image segmentation. *arXiv preprint arXiv:1706.05587*.

[Du, El-Khamy, and Lee 2019] Du, X.; El-Khamy, M.; and Lee, J. 2019. Amnet: Deep atrous multiscale stereo disparity estimation networks. *arXiv preprint arXiv:1904.09099*.

[Gao et al. 2019] Gao, S.-H.; Cheng, M.-M.; Zhao, K.; Zhang, X.-Y.; Yang, M.-H.; and Torr, P. 2019. Res2net: A new multi-scale backbone architecture. *arXiv preprint arXiv:1904.01169*.

[Guo et al. 2019] Guo, X.; Yang, K.; Yang, W.; Wang, X.; and Li, H. 2019. Group-wise correlation stereo network. 3273–3282.

[Huang et al. 2017] Huang, G.; Liu, Z.; Van Der Maaten, L.; and Weinberger, K. Q. 2017. Densely connected convolutional networks. In *Proceedings of the IEEE conference on computer vision and pattern recognition*, 4700–4708.

[Kendall et al. 2017] Kendall, A.; Martirosyan, H.; Dasgupta, S.; Henry, P.; Kennedy, R.; Bachrach, A.; and Bry, A. 2017. End-to-end learning of geometry and context for deep stereo regression. In *Proceedings of the IEEE International Conference on Computer Vision*, 66–75.

[Long, Shelhamer, and Darrell 2015] Long, J.; Shelhamer, E.; and Darrell, T. 2015. Fully convolutional networks for semantic segmentation. In *Proceedings of the IEEE conference on computer vision and pattern recognition*, 3431–3440.

[Luo, Schwing, and Urtasun 2016] Luo, W.; Schwing, A. G.; and Urtasun, R. 2016. Efficient deep learning for stereo matching. In *Proceedings of the IEEE Conference on Computer Vision and Pattern Recognition*, 5695–5703.

[Mayer et al. 2016] Mayer, N.; Ilg, E.; Hausser, P.; Fischer, P.; Cremers, D.; Dosovitskiy, A.; and Brox, T. 2016. A large dataset to train convolutional networks for disparity, optical flow, and scene flow estimation. In *Proceedings of the IEEE Conference on Computer Vision and Pattern Recognition*, 4040–4048.

[Schops et al. 2017] Schops, T.; Schonberger, J. L.; Galliani, S.; Sattler, T.; Schindler, K.; Pollefeys, M.; and Geiger, A. 2017. A multi-view stereo benchmark with high-resolution images and multi-camera videos. In *Proceedings of the IEEE Conference on Computer Vision and Pattern Recognition*, 3260–3269.

[Seki and Pollefeys 2017] Seki, A., and Pollefeys, M. 2017. Sgm-nets: Semi-global matching with neural networks. In *Proceedings of the IEEE Conference on Computer Vision and Pattern Recognition*, 231–240.

[Song et al. 2018] Song, X.; Zhao, X.; Hu, H.; and Fang, L. 2018. Edgestereo: A context integrated residual pyramid network for stereo matching. In *Asian Conference on Computer Vision*, 20–35. Springer.

[Song et al. 2019] Song, X.; Zhao, X.; Fang, L.; and Hu, H. 2019. Edgestereo: An effective multi-task learning network for stereo matching and edge detection. *arXiv preprint arXiv:1903.01700*.

[Yang et al. 2018a] Yang, G.; Zhao, H.; Shi, J.; Deng, Z.; and Jia, J. 2018a. Segstereo: Exploiting semantic information

for disparity estimation. In *Proceedings of the European Conference on Computer Vision (ECCV)*, 636–651.

[Yang et al. 2018b] Yang, M.; Yu, K.; Zhang, C.; Li, Z.; and Yang, K. 2018b. Denseaspp for semantic segmentation in street scenes. In *Proceedings of the IEEE Conference on Computer Vision and Pattern Recognition*, 3684–3692.

[Yu et al. 2017] Yu, Z.; Feng, C.; Liu, M.-Y.; and Rama-lingam, S. 2017. Casenet: Deep category-aware semantic edge detection. In *Proceedings of the IEEE Conference on Computer Vision and Pattern Recognition*, 5964–5973.

[Zbontar, LeCun, and others 2016] Zbontar, J.; LeCun, Y.; et al. 2016. Stereo matching by training a convolutional neural network to compare image patches. *Journal of Machine Learning Research* 17(1-32):2.

[Zhong, Dai, and Li 2017] Zhong, Y.; Dai, Y.; and Li, H. 2017. Self-supervised learning for stereo matching with self-improving ability. *arXiv preprint arXiv:1709.00930*.